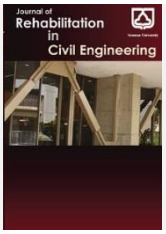

Journal of Rehabilitation in Civil Engineering

Journal homepage: https://civiljournal.semnan.ac.ir/

Impact of rigid and semi-rigid connections on dual-steel frames with various bracing systems using non-linear dynamic analysis

Hossein Khosravi [1]; Mohammad Bahram [2,*]; Mahdiye Shahri [3]

1. Assistant Professor, Department of Civil Engineering, Hakim Sabzevari University, Sabzevar, Iran
2. Department of Civil Engineering, Hakim Sabzevari University, Sabzevar, Iran
3. Department of Civil Engineering, Neyshabur Branch, Islamic Azad University, Neyshabur, Iran

* Corresponding author: *h.khosravi@hsu.ac.ir*

ARTICLE INFO

Article history:
Received: 12 September 2025
Revised: 06 December 2025
Accepted: 23 December 2025

Keywords:
Semi-rigid Connections;
Dual Systems;
Non-linear Dynamic Analysis.

ABSTRACT

During the occurrence of various earthquakes, the formation of local cracks in the connections of the steel frames is regarded as a main problem. Hence, scholars have paid a special attention to the application of steel frames with semi-rigid connections. So far, the frames with semi-rigid connections are rarely utilized, which is mainly due to their high drift rate. In the present article, the impact of semi-rigid connections on the dual-steel frames with various bracing systems was assessed using non-linear dynamic analysis. For accomplishing the analysis, the PERFORM 3D Software was used and the bilinear models were used for modelling the behavior of frames' members. The parameters investigated include maximum base shear, period, frames' drift and energy depreciation of dual systems. The obtained results indicated that the semi-rigid connections lead to decrease in the base shear, while the braces of dual system compensate the increase of drift resulted from utilization of semi-rigid connections.

E-ISSN: 2345-4423

How to cite this article:
Khosravi, H., Shahri, M. and Bahram, M. (2026). Impact of rigid and semi-rigid connections on dual-steel frames with various bracing systems using non-linear dynamic analysis. Journal of Rehabilitation in Civil Engineering, 14(3), 2442. https://doi.org/10.22075/jrce.2025.2442

1. Introduction

For a structure to safely resist lateral loads, it must possess two essential characteristics: adequate stiffness and sufficient ductility. Among the various seismic-resisting systems, moment-resisting frames are widely used in earthquake-prone regions because they are relatively easy to construct and offer high ductility. One of the key components governing the behavior of such systems is the beam-to-column connection, which directly influences the overall stiffness and ductility of the structure. In conventional analyses of steel frames, beam-to-column connections are typically idealized as either perfectly rigid or perfectly pinned. However, in reality, connection behavior lies between these two idealized limits, exhibiting partial rotational stiffness and nonlinear characteristics [1]. Therefore, accounting for the semi-rigid behavior of connections is essential for more realistic and economical structural analysis. In Ref.[2], the investigation of steel moment-resisting frames damaged during the Northridge earthquake revealed that most failures were concentrated in the beam-to-column connection regions. One of the main causes of this damage was the high stress concentration at welded rigid connections and their limited ductility. Following these observations, the use of semi-rigid connections was proposed as an effective alternative. Pulse-type ground motions, which transfer large amounts of energy over short durations, often caused brittle fractures in rigid joints. Due to their limited flexibility, welded rigid connections can dissipate only a small portion of the input energy, whereas semi-rigid connections—with their inherent rotational flexibility—are capable of absorbing and redistributing energy more effectively throughout the structure. Consequently, frames with semi-rigid connections generally demonstrate improved seismic performance compared with those employing rigid connections [3]. Semi-rigid connections can undergo controlled inelastic rotations, thereby reducing the moment transferred from beams to columns by limiting the connection moment capacity and enhancing their plastic rotation capacity. This behavior results in a more favorable redistribution of internal forces and reduces peak bending moments in beams compared with rigidly connected frames. However, semi-rigid frames typically exhibit larger interstory drifts due to their reduced stiffness, and they may experience a modest decrease in overall lateral resistance. From an economic perspective, semi-rigid connections also provide significant advantages due to simpler fabrication and satisfactory seismic behavior; previous studies have reported up to a 20% reduction in total construction costs when semi-rigid connections are used in moment frames. Nevertheless, the relatively large interstory drifts observed in tall semi-rigid frames remain a key limitation, and some researchers recommend combining rigid and semi-rigid connections to control drift while maintaining favorable energy dissipation characteristics [4]. On the positive side, semi-rigid connections are easier and less costly to repair after an earthquake compared with welded rigid joints [5].In addition, modern seismic design approaches often utilise dual structural systems, which combine a moment-resisting frame with bracing elements and may incorporate semi-rigid beam-to-column connections. The use of such systems offers several advantages, particularly in improving the overall lateral stiffness and reducing seismic demands on the moment-resisting frame. In a dual system, a significant portion of the lateral drift is controlled by the bracing members, which enhances the global stability and ductility of the structure. This characteristic makes dual frames superior to conventional moment-resisting frames, especially when semi-rigid connections are considered, as these connections provide a more economical and flexible alternative to fully rigid joints. According to structural design codes and standards, beam-to-column connections are generally classified into three categories based on their rotational stiffness**:** rigid connections with stiffness greater than 90% of a fully rigid joint, pinned (hinged) connections with stiffness less than 20%, and semi-rigid connections with stiffness ranging between 20% and 90% of a rigid connection. The application of semi-rigid connections in dual systems can therefore effectively balance strength, ductility, and cost-efficiency, making them a practical option for modern earthquake-resistant steel structures. Another important characteristic that governs the behavior and failure mechanism of a frame is the connection strength. In general, during an earthquake, by controlling the yield moment capacity of the connections in each frame, it can be ensured that yielding initiates in the

connections before the main structural members, thereby helping the frame to maintain an overall elastic–plastic response. This characteristic can therefore be considered as one of the key indicators for predicting the seismic behavior of a structure [6]. Previous studies have also shown that a portion of the energy transmitted to the structure during strong ground motions is dissipated through damping effects and nonlinear hysteretic behavior.

$$E_i=E_k+E_\xi+E_s+E_h \quad (1)$$

Equation (1) represents the energy balance of a structure, where E_i denotes the input energy from the earthquake, E_k is the kinetic energy, E_ξ represents the viscous damping energy, E_s is the elastic strain energy, and E_h denotes the hysteretic energy [7]. As shown, the total input energy is dissipated through four mechanisms. In general, the kinetic and elastic strain components account for a relatively small portion of the total energy dissipation, whereas the majority is dissipated through damping and yielding mechanisms. The viscous damping energy (E_ξ) is the portion of the input energy that not only contributes to structural damage reduction but also decreases the proportion of hysteretic energy, which is a desirable aspect in the energy balance. Hysteretic energy (E_h) is defined as the energy dissipated through the inelastic behavior of structural members after yielding. Because hysteretic energy is directly related to structural damage, it is considered the most critical component of the energy equation.

The total input, absorbed, and dissipated energies collectively represent the structure's overall response to seismic excitation, although they do not fully describe its detailed behavioral characteristics. Several studies have investigated the seismic performance of steel frames with rigid and semi-rigid connections as well as different bracing systems. For instance, [8] analyzed the seismic behavior of rigid and semi-rigid steel moment-resisting frames under earthquake loading and showed that using semi-rigid connections—while reducing the initial stiffness—can enhance energy dissipation and ductility. In evaluating seismic performance factors, [9] examined a modular corner-supported bracing system and quantitatively determined the response modification factor and other seismic parameters. Moreover, [10] developed improved criteria for the balanced design of X-braced moment-resisting frames, emphasizing the importance of optimal stiffness and ductility distribution within the structure.

In the field of dual structural systems, [11] investigated the seismic performance of dual frames incorporating buckling-restrained braces (BRBs) and semi-rigid connections, demonstrating that the combination of these two components can significantly enhance the seismic stability of the structure. Furthermore, in a more recent study, [12] examined the influence of the location of semi-rigid connections on the seismic performance of steel frame structures and found that the optimal placement of these connections can considerably affect the overall seismic response of the system. In Ref. [13], steel dual frames equipped with energy-dissipating braces featuring high post-yield stiffness were analyzed. The use of replaceable brace joints and the high energy dissipation capacity of the braces were identified as key advantages of such systems. The high post-yield stiffness of the joints, together with the substantial elastic deformation capacity of the moment-resisting frame, results in a significant reduction in story drifts. In Ref.[14], a novel drift-based approach for the seismic design of semi-rigid steel frames was proposed. This method assumes that plastic deformations are primarily concentrated in the semi-rigid connections, while beams and columns remain largely elastic. Recent studies have focused on enhancing the seismic performance of steel moment-resisting frames through retrofitting techniques and advanced damping systems. For instance, Nouri et al. [15] investigated the seismic retrofit of steel moment frames using arc and ring yielding dampers, providing a probabilistic loss assessment based on FEMA P-58. Their study highlights the effectiveness of these dampers in reducing potential damage and energy dissipation during seismic events. In a subsequent study, Nouri et al. [16] conducted a comprehensive seismic performance assessment of steel MRFs retrofitted with arc and ring dampers. This work evaluated key parameters such as inter-story drift, base shear, and energy dissipation, offering insights into the interaction between semi-rigid connections and damping devices under non-linear

dynamic analysis. These recent contributions provide updated evidence on performance-based design strategies and inform the understanding of how retrofitting and damping techniques can optimize the seismic behavior of steel frames, complementing previous research on dual-steel frames with semi-rigid connections and various bracing systems.

2. Methodology

In the present study, the seismic performance of dual steel frames was investigated using nonlinear static (pushover) and nonlinear time-history dynamic analyses. The frames were braced with eccentric inverted V-braces, a combination of eccentric V- and inverted V-braces, a combination of concentric V- and inverted V-braces, and two-story X-braces. Each configuration was evaluated twice: once assuming rigid beam-to-column connections, and once considering semi-rigid connections. All models were designed in the 3D environment of ETABS 2015, and the nonlinear static and dynamic analyses were performed on corresponding 2D frames using PERFORM-3D software [17]. PERFORM-3D, developed by Computers and Structures, Inc. (CSI) [18], provides specialized features for the seismic design and performance evaluation of structures. Two models with 5 and 10 stories, each having three bays, were analyzed, with the middle bay braced. The story height was 3.2 m and the bay length was 5.0 m. The link beam length was 1.0 m. The dead, live, and partition loads were 450 kg/m², 200 kg/m², and 100 kg/m², respectively. The roof dead and roof live loads were 450 kg/m² and 150 kg/m². The wall and parapet loads were 600 kg/m and 300 kg/m, respectively. A Peak Ground Acceleration (PGA) of 0.35 g was assumed for the design earthquake, and the site was classified as Soil Type 2 with 5% damping. The effects of P–Δ were also considered. Three recorded accelerograms—Northridge (PGA = 0.185 g), Chi-Chi06 (PGA = 0.0259 g), and Chi-Chi03 (PGA = 0.0593 g)—were employed for the time-history analyses, with a time step of 0.005 s. For the semi-rigid connections, the resisting moment capacity was assumed to be 50% of the beam's plastic section modulus, and the rotational stiffness of the connections was determined using Equation (2).

$$K_{\theta} = \frac{M_{CE}}{\theta_y} \quad (2)$$

$$M_{CE} = Z.F_{ye} \quad (3)$$

In equations (1) and (2), M_{CE} denotes the expected resisting moment of the connections, Z refers to the plastic section modulus, and F_{ye} represents the expected yield strength, which is equal to $1.1F_y$. To model the behavior of semi-rigid connections, the moment–rotation relationship provided by FEMA 356 [19] was used, assuming the yielding rotation (θ_y) to be 0.003 radians. Various section profiles were employed in the modeling, including IPE sections for beams, HE (IPB) sections for columns, and UNP sections for braces. The steel material was assumed to be St37. The beam layout of all models is shown in Figure 1, while the frame located on axis 1 was selected for nonlinear analysis, and its elevation view is illustrated in Figure 2. In this figure, the abbreviations used for different dual frame configurations are defined as follows: 8EBF represents a dual frame with eccentric inverted V-braces; 7–8EBF denotes a dual frame with eccentric two-story X-braces (V or inverted-V braces); X corresponds to a dual frame with X-braces; 8CBF refers to a dual frame with concentric inverted V-braces; 7–8CBF indicates a dual frame with concentric two-story X-braces (V or inverted-V braces); and 7–8CBF-10St represents a 10-story dual frame with concentric two-story X-braces.

The yielding rotation of $\theta y = 0.003$ rad for the semi-rigid connections was adopted following FEMA 356 recommendations and previous experimental studies. This value represents realistic semi-rigid behavior, and the results are moderately sensitive to its variations: a lower θy leads to faster yielding and a softer frame, while a higher θy produces stiffer behavior closer to rigid connections. It should also be noted that while semi-rigid connections reduce local damage in beams and columns by allowing some rotation and

energy dissipation, they simultaneously decrease the overall frame stiffness and lateral resistance. This highlights a trade-off between local damage mitigation and global structural performance, which becomes particularly significant in taller frames.

In eccentric braced frames, link beams are designed to act as energy-dissipating ‘fuse’ elements. They plastically deform under seismic events, while the rest of the frame remains largely elastic, allowing for easy replacement after a major earthquake.

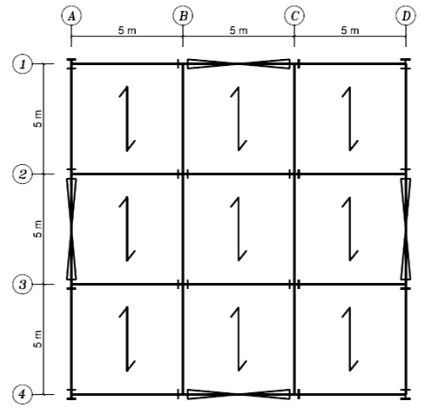

Fig. 1. Positining of beams, column and braces.

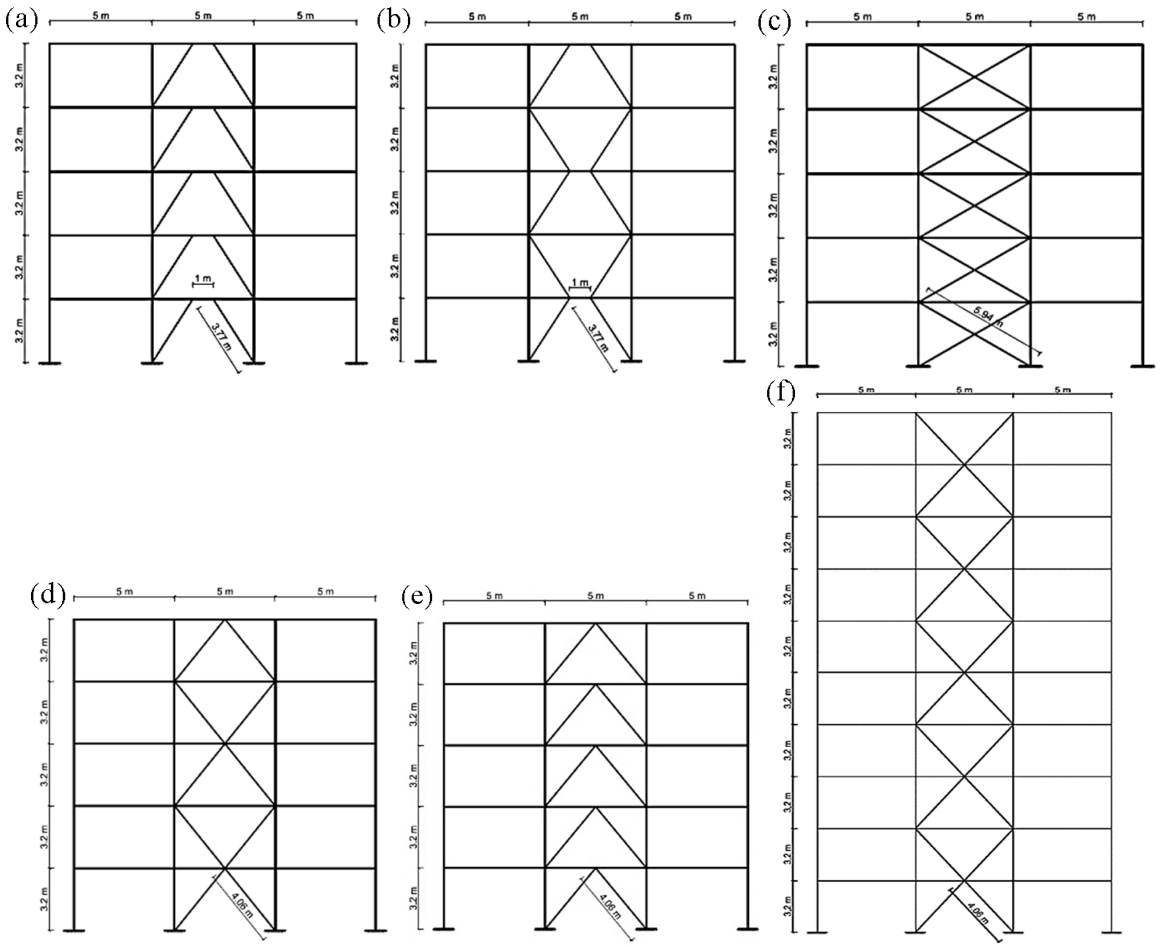

Fig. 2. View of the frame models in different configurations: (a) Dual frame with eccentric inverted V-brace (8-story EBF) (b) Dual frame with eccentric two-story X-brace (V or inverted-V brace) (7–8-story EBF) (c) Dual frame with two-story X-brace (d) Dual frame with concentric inverted V-brace (8-story CBF) (e) Dual frame with concentric two-story X-brace (V or inverted-V brace) (7–8-story CBF) (f) Dual frame with 10-story concentric two-story X-brace (7–8-story CBF–10St).

The frames are designed with regard to the AISC360-10 code and the results are presented in table (1).

Table 1. Designed sections for frames.

	Braces	Beams 1-CD and 1-AB	Beam 1-BC	Columns 1-D and1-A	Columns 1-B and 1-C	Stories
Dual frame with eccentric inverted V-brace	2UNP180	IPE300	IPE400	HE240B	HE320B	1
	2UNP180	IPE300	IPE400	HE240B	HE260B	2
	2UNP160	IPE300	IPE360	HE240B	HE260B	3
	2UNP160	IPE270	IPE270	HE220B	HE240B	4
	2UNP120	IPE240	IPE240	HE220B	HE240B	5
Dual frame with eccentric two-story X-brace (V or inverted-V brace)	2UNP140	IPE300	IPE450	HE200B	HE360B	1
	2UNP140	IPE300	IPE300	HE200B	HE360B	2
	2UNP140	IPE300	IPE400	HE180B	HE200B	3
	2UNP120	IPE300	IPE300	HE180B	HE200B	4
	2UNP100	IPE240	IPE270	HE180B	HE180B	5
Dual frame with X-brace	2UNP140	IPE300	IPE300	HE180B	HE360B	1
	2UNP140	IPE300	IPE300	HE180B	HE280B	2
	2UNP120	IPE300	IPE300	HE180B	HE220B	3
	2UNP120	IPE300	IPE300	HE180B	HE180B	4
	2UNP100	IPE270	IPE270	HE180B	HE180B	5
Dual frame with concentric inverted V-brace	2UNP140	IPE270	IPE500	HE180B	HE340B	1
	2UNP140	IPE270	IPE500	HE180B	HE260B	2
	2UNP120	IPE270	IPE450	HE180B	HE200B	3
	2UNP120	IPE270	IPE450	HE180B	HE160B	4
	2UNP100	IPE240	IPE400	HE180B	HE140B	5
Dual frame with concentric two-story X-brace (V or inverted-V brace)	2UNP160	IPE300	IPE300	HE200B	HE340B	1
	2UNP140	IPE300	IPE300	HE200B	HE320B	2
	2UNP140	IPE300	IPE300	HE160B	HE220B	3
	2UNP120	IPE300	IPE300	HE160B	HE180B	4
	2UNP100	IPE240	IPE400	HE160B	HE140B	5
Dual frame with 10-story concentric two-story X-brace	2UNP160	IPE300	IPE300	HE280B	HE800B	1
	2UNP160	IPE300	IPE300	HE280B	HE800B	2
	2UNP160	IPE300	IPE300	HE240B	HE500B	3
	2UNP140	IPE300	IPE300	HE240B	HE450B	4
	2UNP140	IPE240	IPE400	HE220B	HE320B	5
	2UNP120	IPE300	IPE300	HE220B	HE320B	6
	2UNP120	IPE300	IPE300	HE200B	HE220B	7
	2UNP120	IPE300	IPE300	HE200B	HE220B	8
	2UNP100	IPE300	IPE300	HE160B	HE180B	9
	2UNP100	IPE240	IPE270	HE160B	HE140B	10

3. Validation of numerical modelling

To ensure the accuracy of the numerical modelling and analysis of the frames, the results presented in Ref. [18] were used for verification. In that study, dual steel frames with rigid and semi-rigid connections were evaluated using nonlinear static (pushover) analysis. A comparison between the pushover curve of the dual frame with eccentric inverted V-braces using rigid connections (Rigid-8EBF) obtained in this study and that presented in Ref. [20] (see Figure 3) confirmed the accuracy of the modelling and analysis

procedure. For a more detailed verification, the yielding lateral resistance, ultimate lateral resistance, and stiffness of the initial linear region were compared, and the corresponding values and their percentage differences are summarized in Table 2.

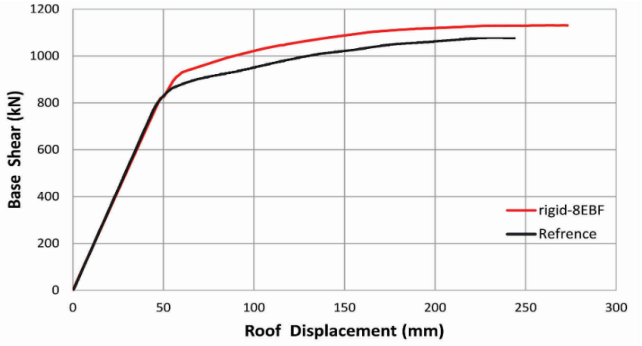

Fig. 3. Comparison of pushover curve (Rigid-8ebf) with reference samples [10].

Table 2. Comparison between reference samples [10] and accomplished samples.

Initial stiffness (slope of the linear region) kN/m	Ultimate strength kN	Yielding strength kN	Validation
18069.8	1107	777	Reference sample
17136.65	1130.62	815	Accomplished samples
5.16	2.13	4.89	Difference percentage

4. Validation of dynamic characteristics (natural period analysis)

4.1. Comparison of structural periods

The following results were obtained from the comparison of the natural periods obtained for the modeled specimens (Tables 3 and 4):

1. The difference between the structural periods corresponding to the first two vibration modes is significantly greater than that of the higher modes. Specifically, the period of the first mode is approximately 2.5 times greater than that of the second mode. This notable difference indicates that the first two modes have a considerable influence on the overall dynamic behavior of the structure.
2. When the beam-to-column connections are modeled as semi-rigid, the structural period increases slightly, reflecting the reduction in the overall stiffness of the system. In other words, a decrease in connection stiffness leads to a marginal increase in the fundamental period.
3. The fundamental period of the structure increases with increasing building height, as expected due to the greater overall flexibility of taller frames.

Table 3. Period for 5-story frames.

Model description	Mode 1	Mode 2	Mode 3	Mode 4	Mode 5
Eccentric inverted V-brace (Rigid)	0.5133	0.2040	0.1237	0.09089	0.06786
Eccentric inverted V-brace (Semi-rigid)	0.5285	0.2095	0.1269	0.09259	0.06829
Concentric inverted V-brace (Rigid)	0.4141	0.1489	0.08888	0.06692	0.05554
Concentric inverted V-brace (Semi-rigid)	0.4187	0.1508	0.08950	0.06716	0.05571
X-brace (Rigid)	0.4140	0.1367	0.07876	0.05844	0.04916
X-brace (Semi-rigid)	0.4188	0.1378	0.07914	0.05859	0.04924
Concentric two-story X-brace (Rigid)	0.4262	0.1493	0.08418	0.06541	0.05268
Concentric two-story X-brace (Semi-rigid)	0.4310	0.1503	0.08446	0.06554	0.05284
Eccentric two-story X-brace (Rigid)	0.5776	0.2094	0.1286	0.07794	0.06055
Eccentric two-story X-brace (Semi-rigid)	0.5898	0.2133	0.1300	0.07832	0.06084

Table 4. Period for 10-story frames.

mode period(sec)	mode 1	mode 2	mode 3	mode 4	mode 5	mode 6	mode 7	mode 8	mode 9	mode 10
7,8CBF-10st-RIGID	0.9464	0.2968	0.1604	0.1098	0.08823	0.0732	0.06325	0.05631	0.04757	0.0359
7,8CBF-10st-SEMI	0.9738	0.3014	0.1621	0.1108	0.08886	0.07363	0.06353	0.05657	0.04776	0.03601

4.2. Comparison of the interstory drift ratios

According to the comparison of the maximum interstory drift ratio diagrams for the studied frames (Figure 4), it is evident that replacing the rigid connections in the dual system with eccentric inverted V-braces by semi-rigid connections reduces the drift in the lower stories but slightly increases it in the upper stories. In the dual system with eccentric two-story X-braces (V or inverted-V braces), the use of semi-rigid connections leads to an overall increase in the interstory drift of all floors. Eccentric bracing systems generally allow larger lateral drifts due to their lower stiffness and the early plastification of the link beams, which makes the drift of dual systems with eccentric braces greater than that of those with concentric braces. For the 5-story dual systems with concentric braces, replacing rigid with semi-rigid connections causes a small increase in drift, mainly due to the higher rotation capacity of semi-rigid joints. However, this increase is not significant because the brace stiffness dominates over the frame stiffness. In the 10-story dual system with concentric two-story X-braces, replacing rigid connections with semi-rigid ones reduces the drift of all stories except for the sixth story. This behavior results from a more uniform distribution of internal forces and a better interaction between members in the semi-rigid condition. According to FEMA 356, the allowable interstory drift ratio for moment-resisting frames corresponding to Immediate Occupancy (IO) and Life Safety (LS) performance levels are 0.7% and 2.5%, respectively. It was observed that the interstory drift ratios of all analyzed frames remained within the Life Safety range.

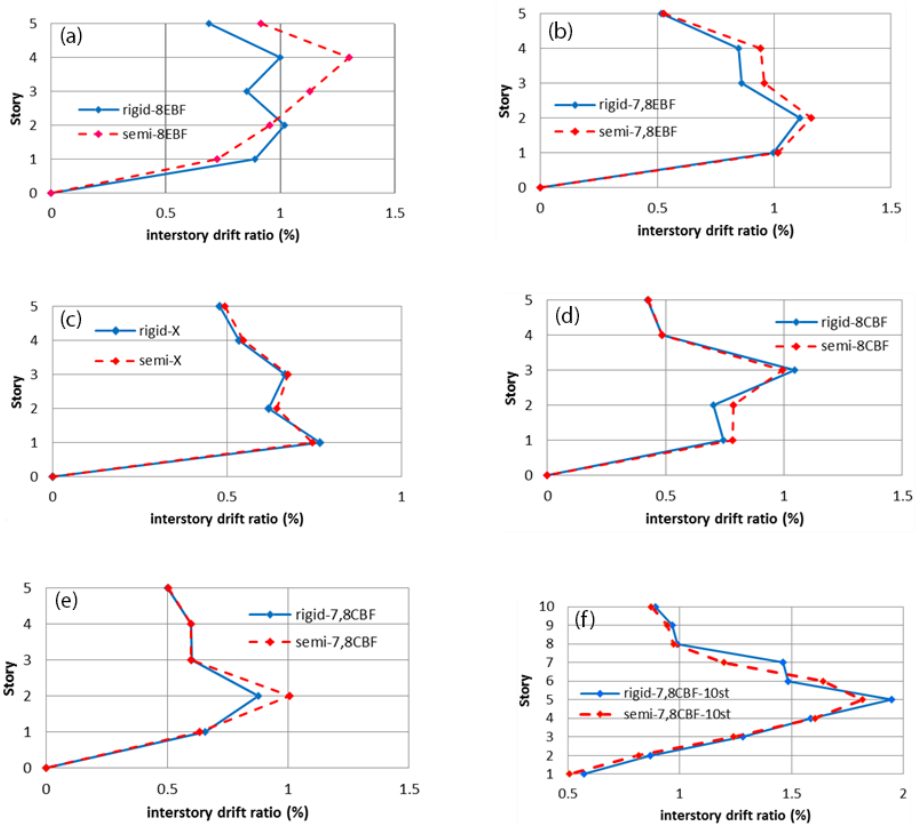

Fig. 4. Comparison of the maximum interstory drift ratios of the floors in the following frames: (a) Dual frame with eccentric inverted V-brace (b) Dual frame with eccentric two-story X-brace (V or inverted-V brace) (c) Dual frame with two-story X-brace (d) Dual frame with concentric inverted V-brace (e) Dual frame with concentric two-story X-brace (V or inverted-V brace) (f) Dual frame with 10-story concentric two-story X-brace.

4.3. Base shear comparison

During an earthquake, lateral forces are transferred through the structure as shear forces, with the maximum shear typically occurring at the base story. These forces are resisted primarily by the seismic load-resisting systems, including the braced frames and the moment-resisting frames. Therefore, evaluating the base shear at the first-story columns is essential to assess the seismic performance of the system.

The results for the maximum base shear of the studied frames are presented in Figure 5. As shown, dual frames with concentric braces exhibit higher base shear values compared to those with eccentric braces, indicating that greater frame stiffness results in higher shear demand. The replacement of rigid connections with semi-rigid ones leads to a reduction in base shear in all cases. This occurs because the semi-rigid behavior of connections decreases the overall stiffness and allows more energy to be dissipated through the nonlinear deformation of members, thereby distributing energy dissipation throughout the structure and reducing shear concentration.

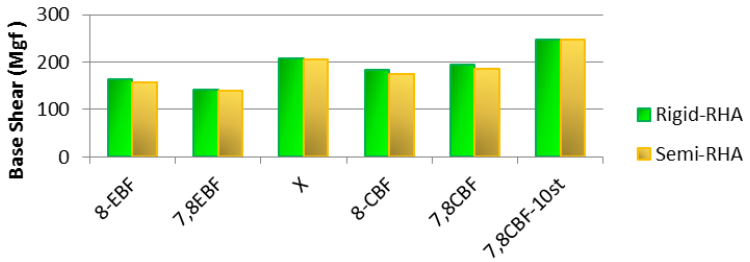

Fig. 5. Maximum base shear in the rigid and semi-rigid samples.

4.4. Energy dissipation by structural members

For this purpose, a detailed categorization of elements at each floor was performed in the PERFORM-3D software, and the corresponding results of the energy dissipated by the structure were obtained after analyzing the frames under gravity and earthquake loading. The results indicated that in dual systems with eccentric braces, the majority of the energy dissipation occurs in the link beams, whereas in dual systems with concentric braces, most of the energy is dissipated by the braces themselves. Replacing rigid connections with semi-rigid ones increases the total amount of energy dissipated by both braces and link beams. Figure 6 presents the amount of hysteretic energy dissipated in each story of the analyzed frames. A comparison of these diagrams shows that the maximum energy dissipation due to earthquake excitation occurs mainly in the first and second stories, and the replacement of rigid connections with semi-rigid ones has no significant influence on the total hysteretic energy of the structure. In the two-story eccentric braced frame (two-story EBF), where no link beam exists in the second and fourth stories, the energy dissipation is nearly zero. In contrast, in the first and third stories—where link beams connect the braces of the upper and lower stories—the amount of energy dissipated is approximately three times greater than that in the single-story EBF system. In the 10-story dual frame, the highest hysteretic energy dissipation occurs in the middle stories (third to seventh stories). The replacement of rigid connections with semi-rigid ones results in a reduction in hysteretic energy in all stories except the fifth and sixth, due to improved force redistribution. As observed in Figure 6, unlike the two-story EBF system where energy dissipation is concentrated only in two floors, the other frames exhibit a more distributed energy dissipation pattern among the stories. Since hysteretic energy dissipation is directly related to structural damage, it can be concluded that the single-story EBF system shows better seismic performance and lower damage compared with the two-story EBF system. In the 5-story concentric dual frames, the amount of energy dissipation—and consequently, the structural damage—is greater in the lower stories than in the upper ones. Moreover, in the 10-story concentric two-story X-braced frame, the middle stories exhibit significantly higher vulnerability compared with the top and bottom stories.

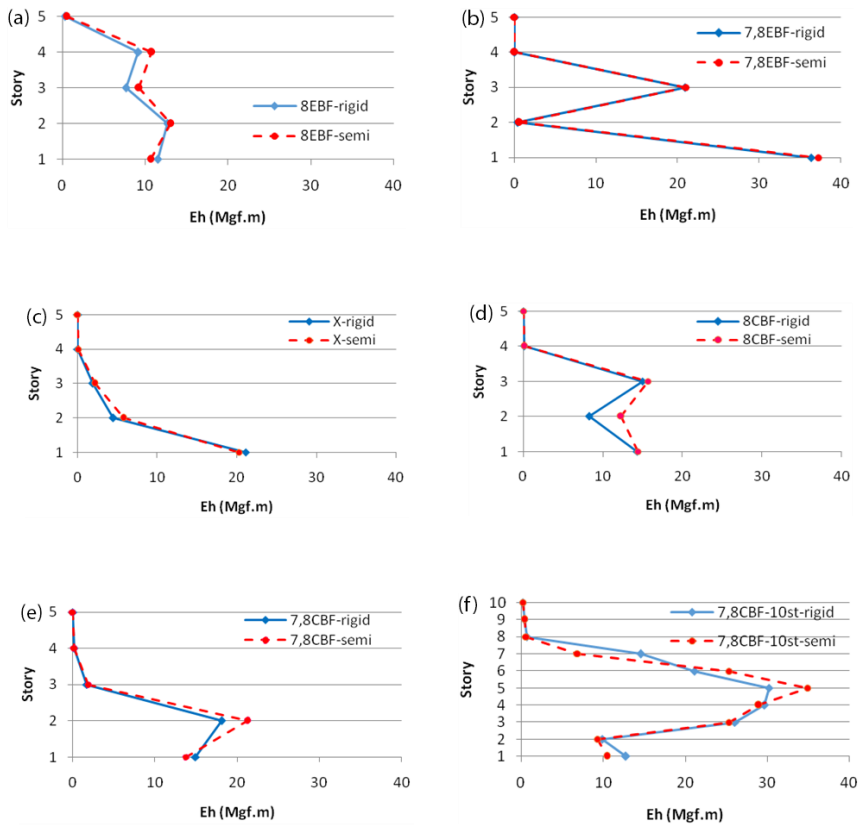

Fig. 6. Dissipated energy of each story in the following frames: (a) Dual frame with eccentric inverted V-brace (b) Dual frame with eccentric two-story X-brace (V or inverted-V brace) (c) Dual frame with two-story X-brace (d) Dual frame with concentric inverted V-brace (e) Dual frame with concentric two-story X-brace (V or inverted-V brace) (f) Dual frame with 10-story concentric two-story X-brace.

To quantify the story-wise distribution of hysteretic energy in the analyzed frames, the results obtained from PERFORM-3D were tabulated. Table 5 presents the story-wise hysteretic energy (Eh) for each frame, showing the comparison between rigid and semi-rigid connections. This tabular representation allows a clear view of how energy dissipation varies across stories and connection types, complementing the observations previously illustrated in Figure 6.

Table 5. Story-wise Hysteretic Energy (Eh) of Analyzed Frames with Rigid and Semi-rigid Connections (Mgf·m).

Frame Type (Fig. 6)	Connection	Story	Eh (Mgf·m)
(a) Dual frame with eccentric inverted V-brace	Rigid	1	12
(a) Dual frame with eccentric inverted V-brace	Rigid	2	13
(a) Dual frame with eccentric inverted V-brace	Rigid	3	8
(a) Dual frame with eccentric inverted V-brace	Rigid	4	9
(a) Dual frame with eccentric inverted V-brace	Rigid	5	0
(a) Dual frame with eccentric inverted V-brace	Semi-rigid	1	11
(a) Dual frame with eccentric inverted V-brace	Semi-rigid	2	14
(a) Dual frame with eccentric inverted V-brace	Semi-rigid	3	9
(a) Dual frame with eccentric inverted V-brace	Semi-rigid	4	11
(a) Dual frame with eccentric inverted V-brace	Semi-rigid	5	0
(b) Dual frame with eccentric two-story X-brace	Rigid	1	37
(b) Dual frame with eccentric two-story X-brace	Rigid	2	1
(b) Dual frame with eccentric two-story X-brace	Rigid	3	21
(b) Dual frame with eccentric two-story X-brace	Rigid	4	0
(b) Dual frame with eccentric two-story X-brace	Rigid	5	0
(b) Dual frame with eccentric two-story X-brace	Semi-rigid	1	38
(b) Dual frame with eccentric two-story X-brace	Semi-rigid	2	1
(b) Dual frame with eccentric two-story X-brace	Semi-rigid	3	21
(b) Dual frame with eccentric two-story X-brace	Semi-rigid	4	0
(b) Dual frame with eccentric two-story X-brace	Semi-rigid	5	0
(c) Dual frame with two-story X-brace	Rigid	1	22

(c) Dual frame with two-story X-brace	Rigid	2	6
(c) Dual frame with two-story X-brace	Rigid	3	2
(c) Dual frame with two-story X-brace	Rigid	4	1
(c) Dual frame with two-story X-brace	Rigid	5	0
(c) Dual frame with two-story X-brace	Semi-rigid	1	21
(c) Dual frame with two-story X-brace	Semi-rigid	2	7
(c) Dual frame with two-story X-brace	Semi-rigid	3	2
(c) Dual frame with two-story X-brace	Semi-rigid	4	1
(c) Dual frame with two-story X-brace	Semi-rigid	5	0
(d) Dual frame with concentric inverted V-brace	Rigid	1	15
(d) Dual frame with concentric inverted V-brace	Rigid	2	9
(d) Dual frame with concentric inverted V-brace	Rigid	3	16
(d) Dual frame with concentric inverted V-brace	Rigid	4	0
(d) Dual frame with concentric inverted V-brace	Rigid	5	0
(d) Dual frame with concentric inverted V-brace	Semi-rigid	1	15
(d) Dual frame with concentric inverted V-brace	Semi-rigid	2	13
(d) Dual frame with concentric inverted V-brace	Semi-rigid	3	17
(d) Dual frame with concentric inverted V-brace	Semi-rigid	4	0
(d) Dual frame with concentric inverted V-brace	Semi-rigid	5	0
(e) Dual frame with concentric two-story X-brace	Rigid	1	15
(e) Dual frame with concentric two-story X-brace	Rigid	2	18
(e) Dual frame with concentric two-story X-brace	Rigid	3	3
(e) Dual frame with concentric two-story X-brace	Rigid	4	1
(e) Dual frame with concentric two-story X-brace	Rigid	5	0
(e) Dual frame with concentric two-story X-brace	Semi-rigid	1	14
(e) Dual frame with concentric two-story X-brace	Semi-rigid	2	22
(e) Dual frame with concentric two-story X-brace	Semi-rigid	3	3
(e) Dual frame with concentric two-story X-brace	Semi-rigid	4	1
(e) Dual frame with concentric two-story X-brace	Semi-rigid	5	0
(f) Dual frame with 10-story concentric two-story X-brace	Rigid	1	12
(f) Dual frame with 10-story concentric two-story X-brace	Rigid	2	10
(f) Dual frame with 10-story concentric two-story X-brace	Rigid	3	26
(f) Dual frame with 10-story concentric two-story X-brace	Rigid	4	30
(f) Dual frame with 10-story concentric two-story X-brace	Rigid	5	31
(f) Dual frame with 10-story concentric two-story X-brace	Rigid	6	22
(f) Dual frame with 10-story concentric two-story X-brace	Rigid	7	16
(f) Dual frame with 10-story concentric two-story X-brace	Rigid	8	2
(f) Dual frame with 10-story concentric two-story X-brace	Rigid	9	1
(f) Dual frame with 10-story concentric two-story X-brace	Rigid	10	0
(f) Dual frame with 10-story concentric two-story X-brace	Semi-rigid	1	11
(f) Dual frame with 10-story concentric two-story X-brace	Semi-rigid	2	9
(f) Dual frame with 10-story concentric two-story X-brace	Semi-rigid	3	25
(f) Dual frame with 10-story concentric two-story X-brace	Semi-rigid	4	29
(f) Dual frame with 10-story concentric two-story X-brace	Semi-rigid	5	36
(f) Dual frame with 10-story concentric two-story X-brace	Semi-rigid	6	26
(f) Dual frame with 10-story concentric two-story X-brace	Semi-rigid	7	8
(f) Dual frame with 10-story concentric two-story X-brace	Semi-rigid	8	2
(f) Dual frame with 10-story concentric two-story X-brace	Semi-rigid	9	1
(f) Dual frame with 10-story concentric two-story X-brace	Semi-rigid	10	0

The tabulated results confirm the observations previously illustrated in Figure 6. In dual frames with eccentric braces, energy dissipation is concentrated primarily in the link beams, whereas in concentric-braced frames, the braces themselves dissipate most of the energy. Replacing rigid connections with semi-rigid ones generally increases the dissipated energy in both braces and link beams, although the effect varies across stories. For example, in the two-story eccentric-braced frames, energy dissipation is nearly zero in stories without link beams, while it peaks in stories where link beams connect the braces. In taller frames, such as the 10-story concentric dual frame, the middle stories exhibit the highest hysteretic energy, reflecting higher vulnerability and potential damage in these regions. Overall, Table 5 provides a clear quantitative view of story-wise energy dissipation for both rigid and semi-rigid connections, facilitating a more detailed comparison among the analyzed frames.

4.5. Damage localization

Figure 7 illustrates the deformed shapes of the analyzed frames under earthquake loading. In this figure, members shown in red indicate elements that have reached the collapse mechanism. It can be observed that in the eccentric braced systems, damage is mainly concentrated in the link beams, whereas in the concentric braced systems, the braces are the primary locations of yielding. Replacing rigid connections with semi-rigid ones in eccentric frames not only affects the link beams but also increases the participation of floor beams in energy dissipation. This indicates that the eccentric system with rigid connections demonstrates better overall performance and damage concentration. In the five-story concentric frames, only the braces have yielded, and the use of semi-rigid connections causes a slight reduction in strength and stiffness, which can be compensated by reinforcing a limited number of members. However, in the ten-story frame with rigid connections, both braces and a considerable number of beams and columns have yielded. When semi-rigid connections are used in the ten-story frame, column yielding is prevented, although the overall stiffness and strength of the frame are significantly reduced. This suggests that the ten-story frame with semi-rigid connections exhibits a weaker seismic performance.

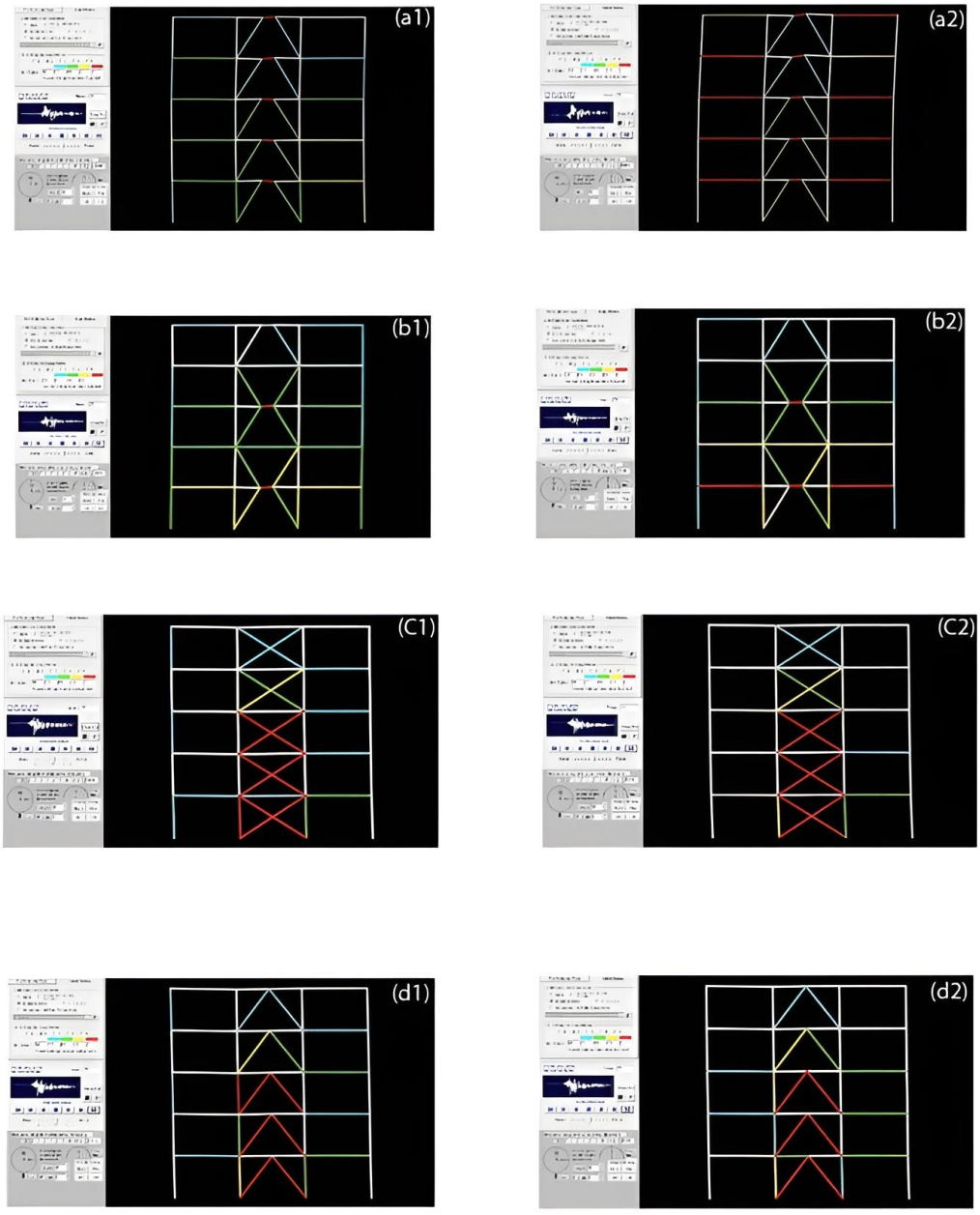

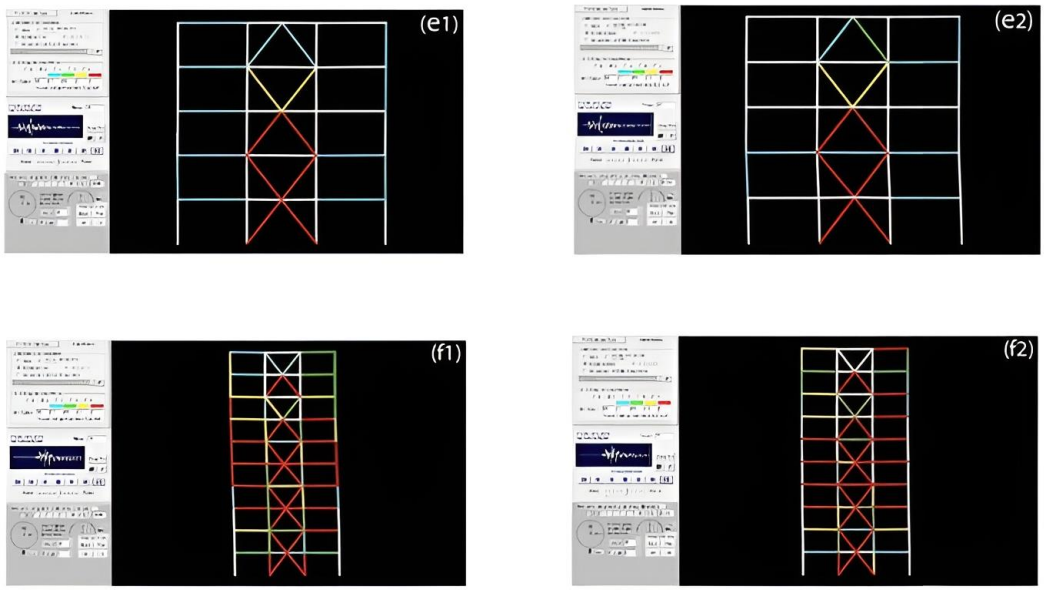

Fig. 7. Location of damages after the earthquake in the following frames: (a1) and (a2): Dual frame with eccentric inverted V-brace (b1) and (b2): Dual frame with eccentric two-story X-brace (V or inverted-V brace) (c1) and (c2): Dual frame with two-story X-brace (d1) and (d2): Dual frame with concentric inverted V-brace (e1) and (e2): Dual frame with concentric two-story X-brace (V or inverted-V brace) (f1) and (f2): Dual frame with 10-story concentric two-story X-brace.

5. Conclusions

The use of semi-rigid connections and the increase in structural height both lead to a longer fundamental period. The influence of building height on the period is more significant than that of the connection rigidity. An increase in the fundamental period makes the structure more flexible under seismic excitations, which in turn reduces the seismic forces acting on it.

The adoption of semi-rigid connections slightly decreases the base shear of the structure and the braces, particularly in dual systems where the presence of braces governs the overall stiffness. The rigidity of beam-to-column connections has little effect on the maximum shear force in the braces, but it does influence the maximum shear force in the columns. Furthermore, due to the high stiffness of the braces, the use of semi-rigid connections does not significantly affect the total hysteretic energy dissipated by the structure.

A comparison of story drifts indicates that in the semi-rigid models, structural displacements increase due to higher connection rotations. However, in dual systems, a large portion of the lateral drift is controlled by the braces, which is an advantage compared to pure moment-resisting frames, especially under semi-rigid connection conditions.

Overall, the use of semi-rigid connections in taller dual-frame structures can be effective, provided that lateral drift is properly controlled and the required strength is ensured.

In tall semi-rigid dual frames, eccentric or combined eccentric-inverted V bracing effectively controls lateral drift while protecting the moment-resisting frame, highlighting key design considerations such as link beam ductility, brace layout, and connection rotational capacity.

Funding

This research did not receive any specific grant from funding agencies in the public, commercial, or not-for-profit sectors.

Conflicts of interest

The authors declare that they have no known competing financial interests or personal relationships that could have appeared to influence the work reported in this paper.

Authors contribution statement

Hossein Khosravi: Methodology, Investigation, Writing – original draft, Funding acquisition.

Mohammad Bahram: Supervision, Writing – review & editing.

Mahdiye Shahri: Conceptualization, Methodology, Writing – review & editing.

References

[1] Patnana V, Vyavahare AY. Moment rotation curves for semi rigid connections. 2016 Int. Conf. Electr. Electron. Optim. Tech., 2016, p. 2563–8.

[2] Feizi MG, Mojtahedi A, Nourani V. Effect of semi-rigid connections in improvement of seismic performance of steel moment-resisting frames. Steel Compos Struct 2015;19:467–84.

[3] Najdian M, Izadinia M. Evaluation of seismic behavior on steel frames with TSW semi-rigid connections under the nonlinear time history analysis. Appl Mech Mater 2012;166:2083–7.

[4] Dubina D, Stratan A, De Matteis G, Landolfo R. Seismic performance of dual steel moment-resisting frames. 2021.

[5] Popa AG, Mathe AE. Performance--based analysis of steel structures with semi-rigid connections. Proc 34th IABSE Symp "Large Struct Ans Infrastructures Environ Constrained Urban Areas" 2010:356–7.

[6] Standardization EC for. Eurocode 3: Design of Steel Structures 2002.

[7] Uang CM, Bertero VV. Evaluation of seismic energy in structures. Earthq Eng Struct Dyn 1990;19:77–90.

[8] Rigi A, JavidSharifi B, Hadianfard MA, Yang TY. Study of the seismic behavior of rigid and semi-rigid steel moment-resisting frames. J Constr Steel Res 2021;186:106910.

[9] Farajian M, Kildashti K, Sharafi P, Eslamnia H. Quantification of seismic performance factors for modular corner-supported steel bracing system. Structures 2022;45:257–74.

[10] Lotfollahi M, Alinia MM, Taciroglu E. Development of Improved Criteria for the Balanced Design of X-braced Moment Resisting Frame Systems. J Build Eng 2025:113158.

[11] Barbagallo F, Bosco M, Marino EM, Rossi PP. Seismic design and performance of dual structures with BRBs and semi-rigid connections. J Constr Steel Res 2019;158:306–16.

[12] E E. Location of semi-rigid connections effect on the seismic performance of steel frame structures. Electron J Struct Eng 2022;22:1–10.

[13] Baiguera M, Vasdravellis G, Karavasilis TL. Dual seismic-resistant steel frame with high post-yield stiffness energy-dissipative braces for residual drift reduction. J Constr Steel Res 2016;122:198–212.

[14] Pirmoz A, Liu MM. Direct displacement-based seismic design of semi-rigid steel frames. J Constr Steel Res 2017;128:201–9.

[15] Nouri Y, Jouneghani HG, Shirkhani A, Hemati E, Hemati SA, Hajirasouliha I. Seismic retrofit of steel moment frames with arc and ring yielding dampers: A probabilistic loss assessment using FEMA P-58. Structures 2025;76:108898.

[16] Nouri Y, Shirkhani A, Jouneghani HG, Hemati E, De Domenico D. Seismic performance assessment of steel MRFs retrofitted with arc and ring dampers. J Constr Steel Res 2026;236:109949.

[17] Inc Computer and Structures. Manual of PERFORM-3D Version 5.0.0 2011.

[18] DC CC of. Nonlinear analysis and performance assessment for 3-D structures (PERFORM-3D) n.d.

[19] FE P. commentary for the seismic rehabilitation of buildings (FEMA356). Washington, DC Fed Emerg Manag Agency 2000;7:518.

[20] Khosravi H, Hejazi Y, Mousavi SS. Analysis of supported steel frames with rigid and semi-rigid connections. Gradevinar 2017;69:131–9.